Electronic Supplementary Information

Manuscript ID NJ-ART-12-2021-006106

Ferrocene functionalized enantiomerically pure Schiff bases and their Zn(II) and Pd(II) complexes : a spectroscopic, crystallographic, electrochemical and computational investigation

Salvador Celedón, Paul Hamon, Vania Artigas, Mauricio Fuentealba, Samia Kahlal, David Carrillo, Jean-Yves Saillard, Jean-René Hamon, Carolina Manzur

Contents Page

Fig. S1 Experimental (top) and simulated (bottom) ion peaks of complex **3**. 2

Fig. S2 Experimental (top) and simulated (bottom) ion peaks of complex **4**. 2

Fig. S3 Experimental (top) and simulated (bottom) ion peaks of bimetallic complex **5**. 2

Fig. S4 Experimental (top) and simulated (bottom) ion peaks of bimetallic complex **6**. 3

Fig. S5 FT-IR solid-state spectra (KBr disk) of half unit **3** (left) and its related complex **5** (right). 3

Fig. S6 FT-IR solid-state spectra (KBr disk) of half unit **4** (left) and its related complex **6** (right). 4

Fig. S7 ^{1}H NMR spectrum of the bimetallic complex **5** recorded in DMSO-d_6 at 298 K. 4

Fig. S8 ^{1}H NMR spectrum of the bimetallic complex **6** recorded in DMSO-d_6 at 298 K. 5

Fig. S9 ^{13}C{^{1}H} NMR spectrum of half unit **3** recorded in DMSO-d_6 at 298 K. 5

Fig. S10 ^{13}C{^{1}H} NMR spectrum of half unit **4** recorded in DMSO-d_6 at 298 K. 6

Fig. S11 ^{13}C{^{1}H} NMR spectrum of the bimetallic complex **6** recorded in DMSO-d_6 at 298 K. 6

Fig. S12 Crystal packing of **4**·^{i}PrOH expanded in the y-axis through H-bond interactions. 7

Fig. S13 Cyclic voltammograms of free ferrocene (top), half unit **3** (middle) and of the bimetallic complex **5** (bottom). 7

Fig. S14. TD-DFT simulated spectra of complexes **3-6.** 8

Table S1 Selected metrical parameters of the ferrocenyl units in compounds **3** and **4**·^{i}PrOH. 8

Table S2 Hydrogen bond interactions in **3** and **4**·^{i}PrOH. 8

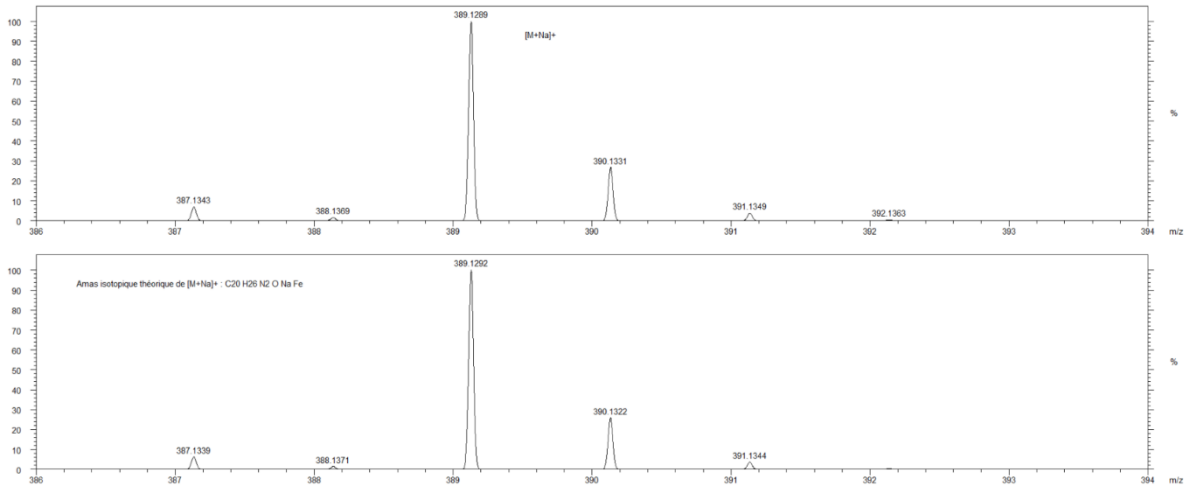

Fig. S1 Experimental (top) and simulated (bottom) ion peaks of complex **3**.

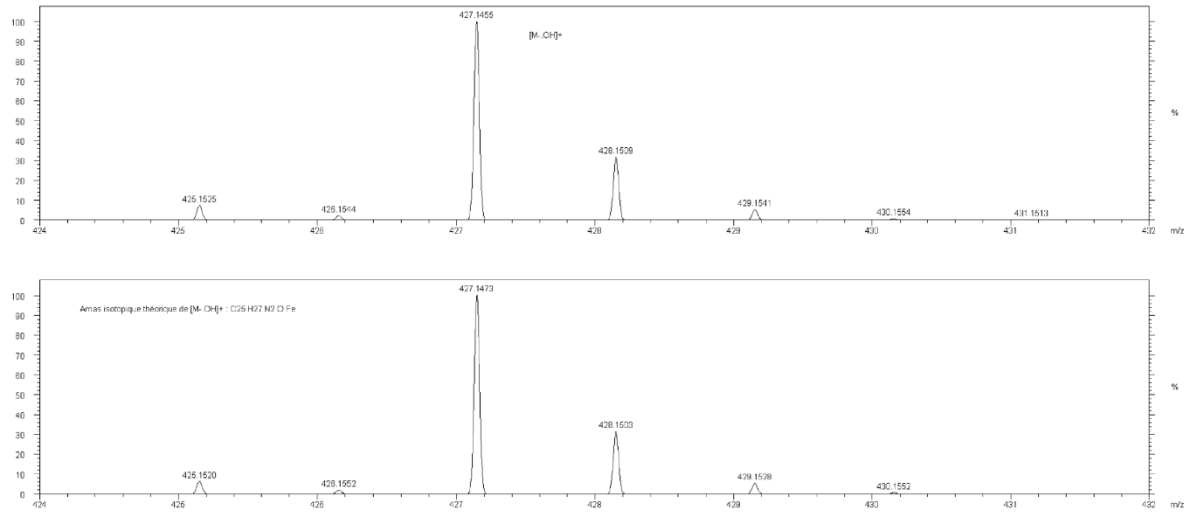

Fig. S2 Experimental (top) and simulated (bottom) ion peaks of complex **4**.

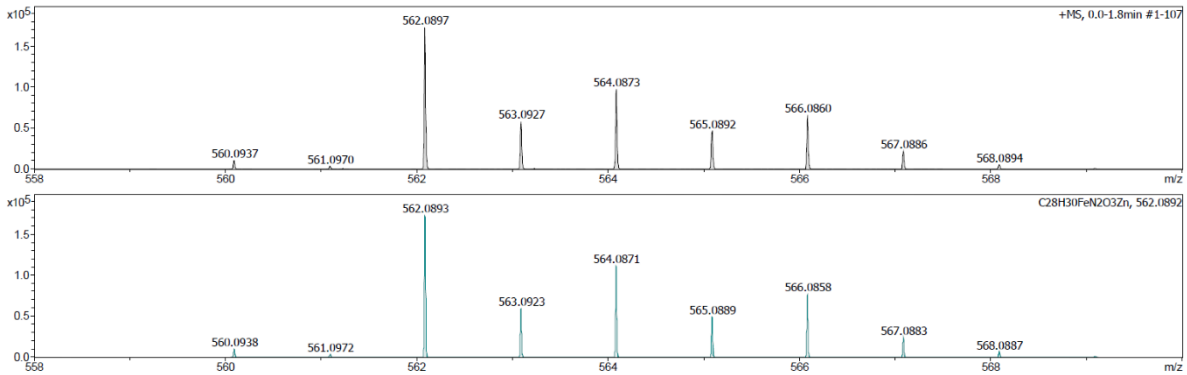

Fig. S3 Experimental (top) and simulated (bottom) ion peaks of the bimetallic complex **5**.

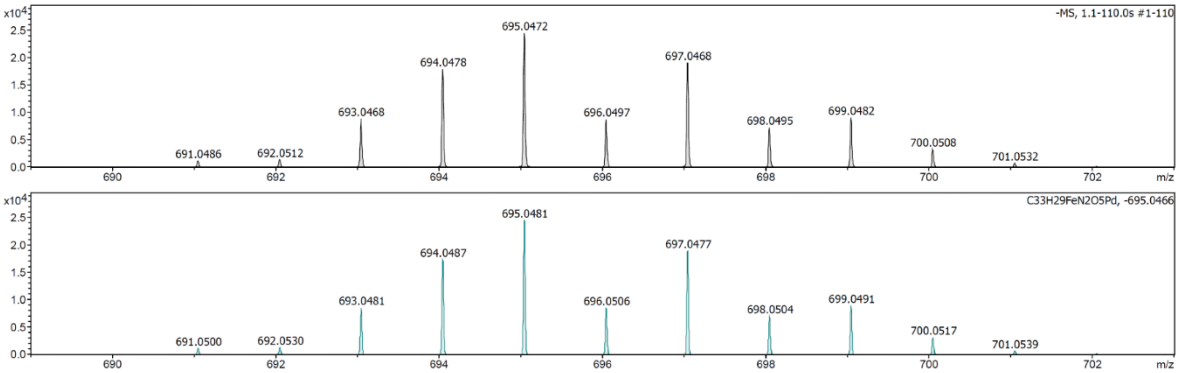

Fig. S4 Experimental (top) and simulated (bottom) ion peaks of the bimetallic complex **6**.

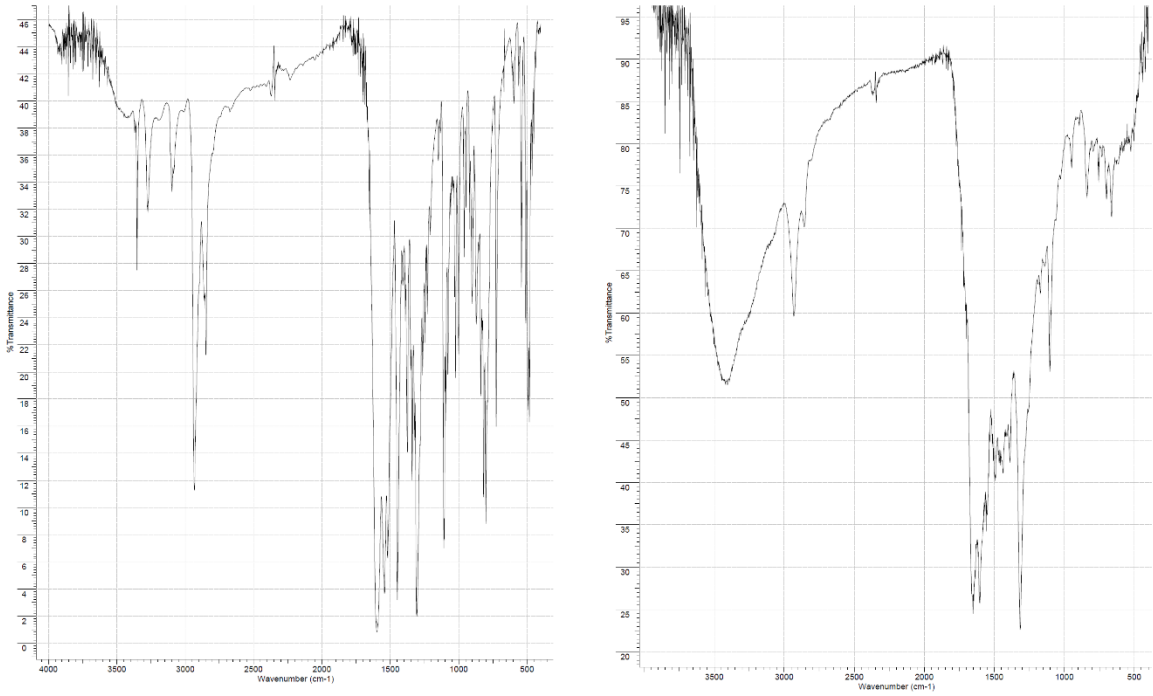

Fig. S5 FT-IR solid-state spectra (KBr disk) of half unit **3** (left) and its related complex **5** (right).

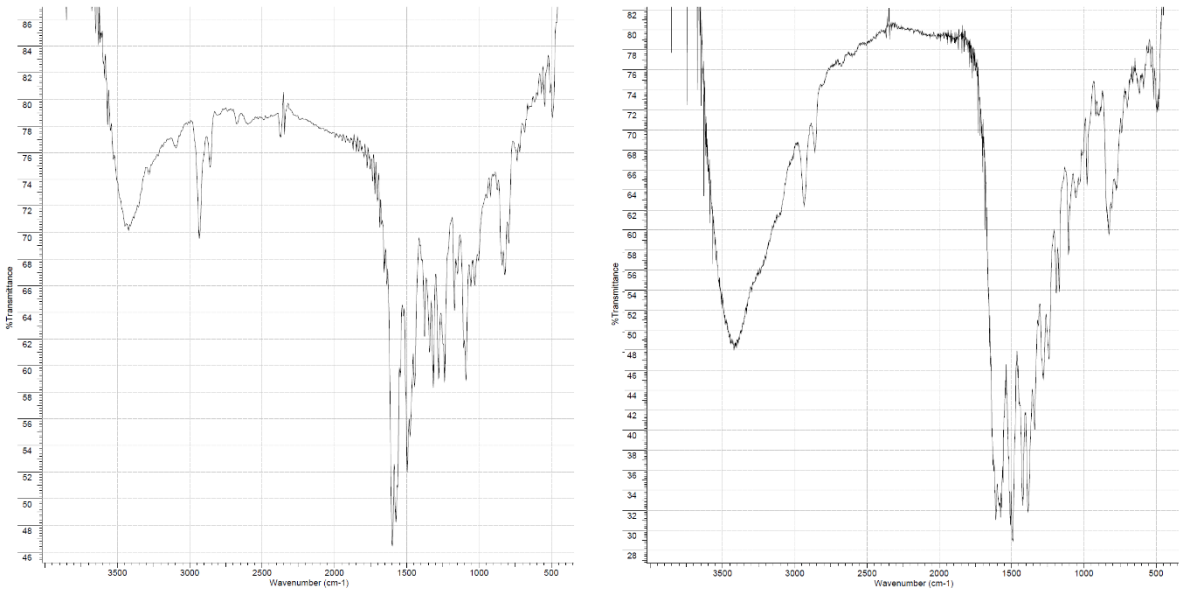

Fig. S6 FT-IR solid-state spectra (KBr disk) of half unit **4** (left) and its related complex **6** (right).

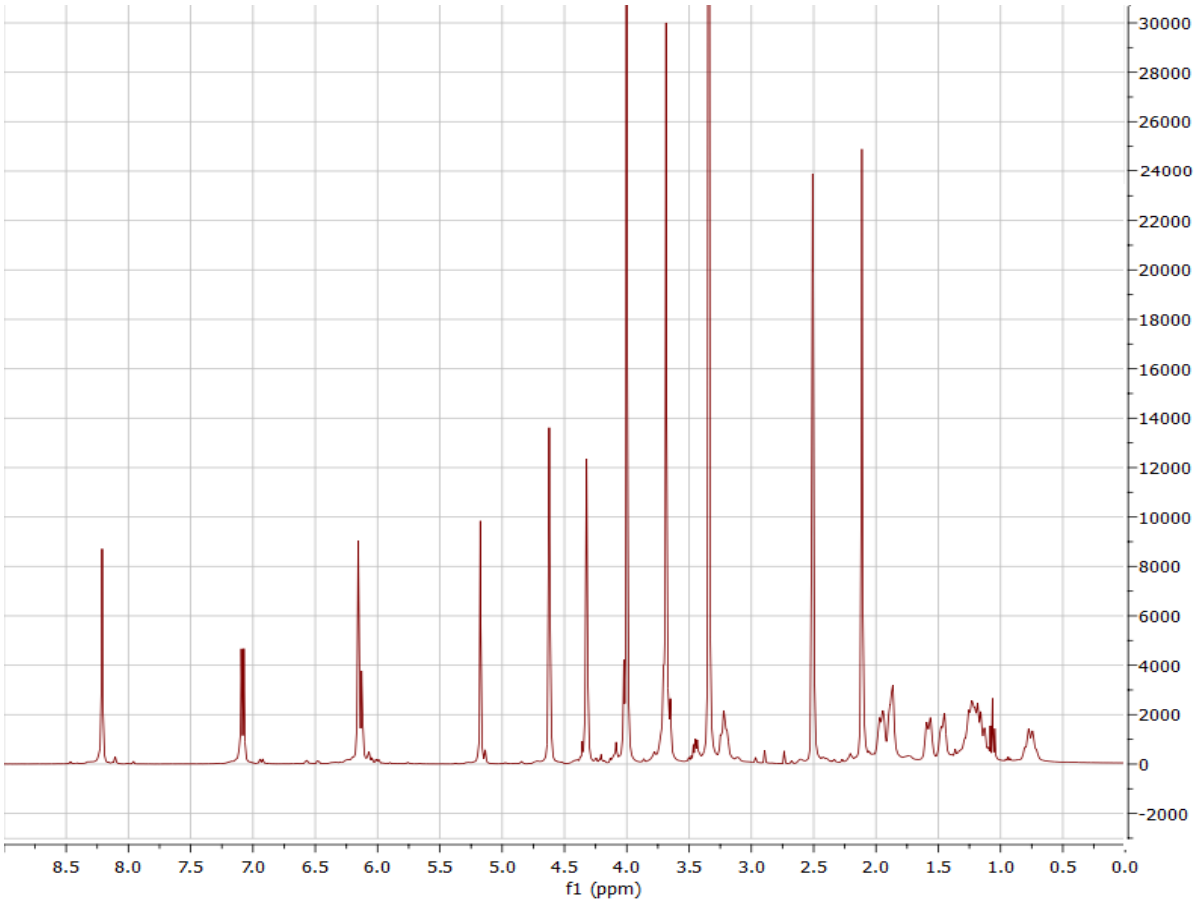

Fig. S7 ^{1}H NMR spectrum of bimetallic complex **5** recorded in DMSO-d_6 at 298 K.

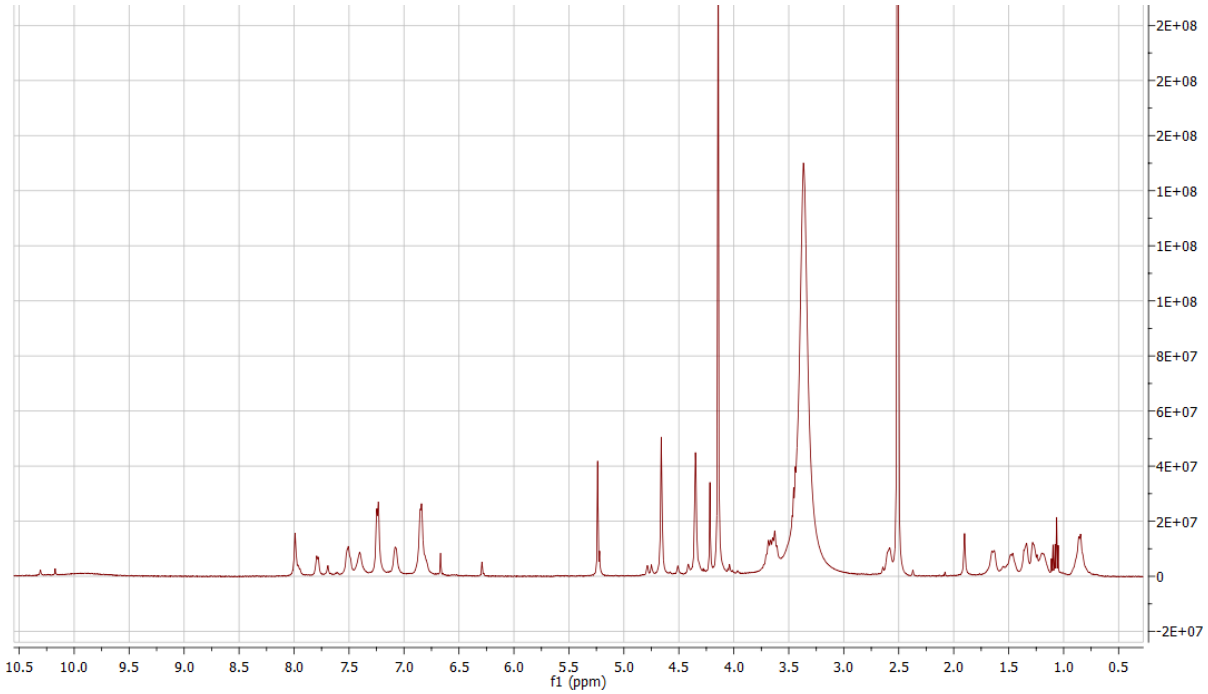

Fig. S8 ^{1}H NMR spectrum of bimetallic complex **6** recorded in DMSO-d_6 at 298 K.

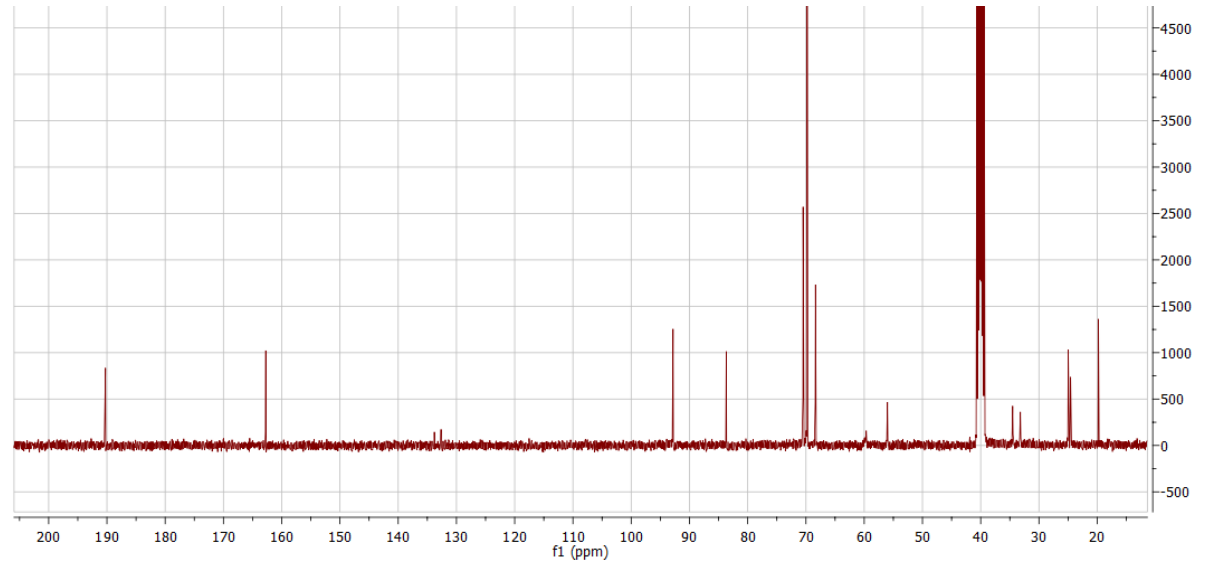

Fig. S9 ^{13}C{^{1}H} NMR spectrum of complex **3** recorded in DMSO-d_6 at 298 K.

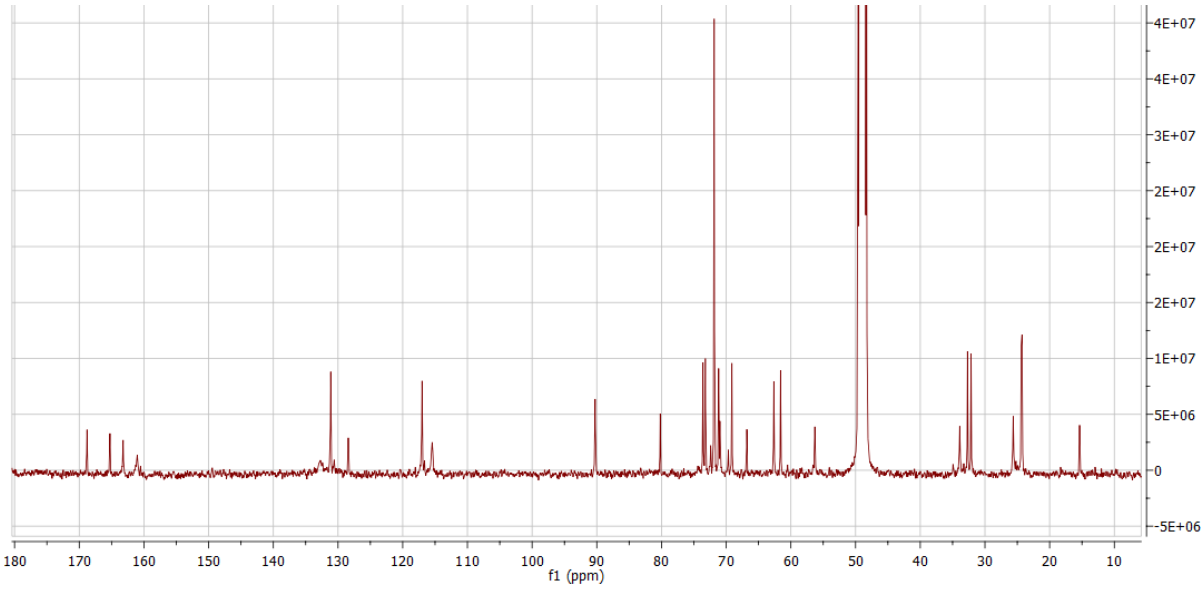

Fig. S10 $^{13}C\{^{1}H\}$ NMR spectrum of complex **4** recorded in DMSO-d_6 at 298 K.

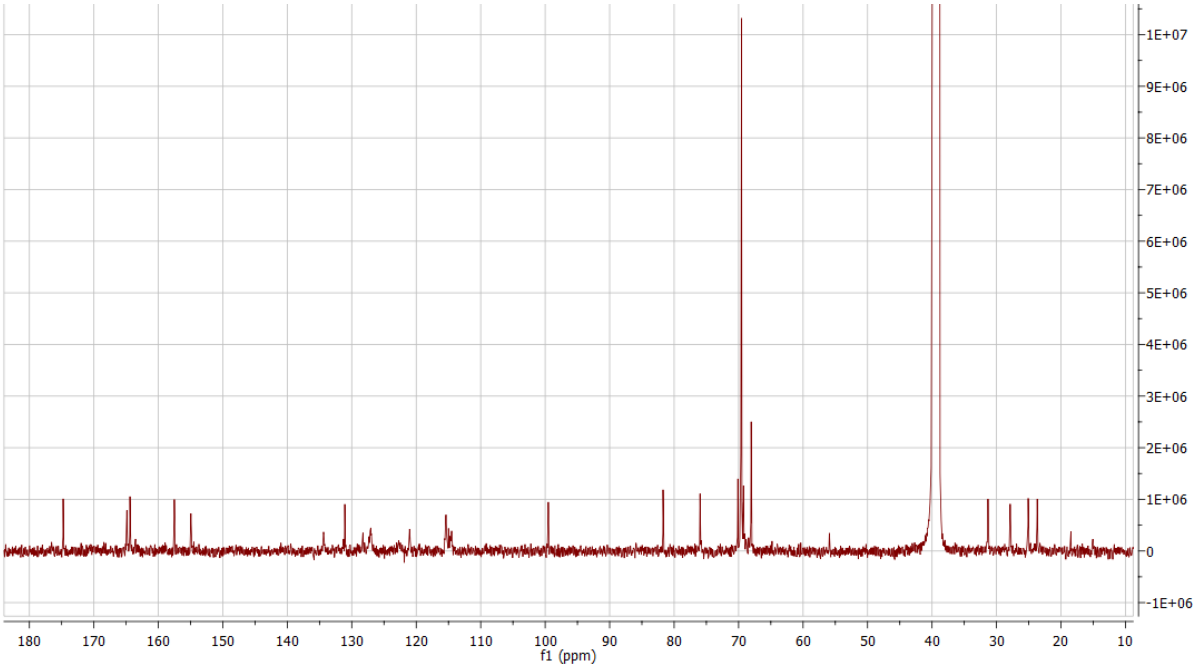

Fig. S11 $^{13}C\{^{1}H\}$ NMR spectrum of bimetallic complex **6** recorded in DMSO-d_6 at 298 K.

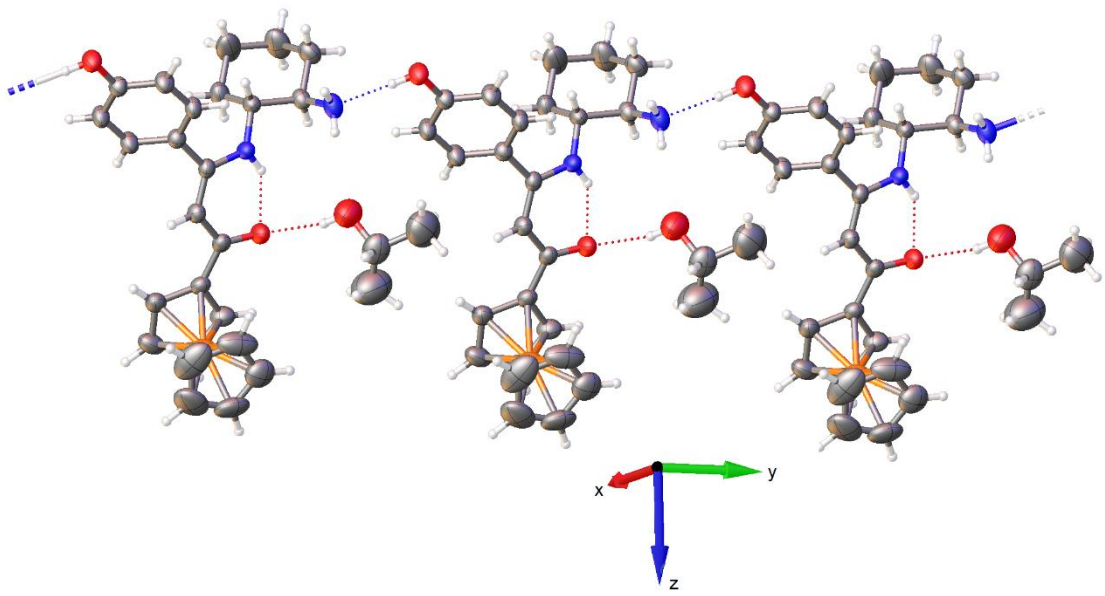

Fig. S12 Crystal packing of **4**·^{i}PrOH expanded in the y-axis through H-bond interactions.

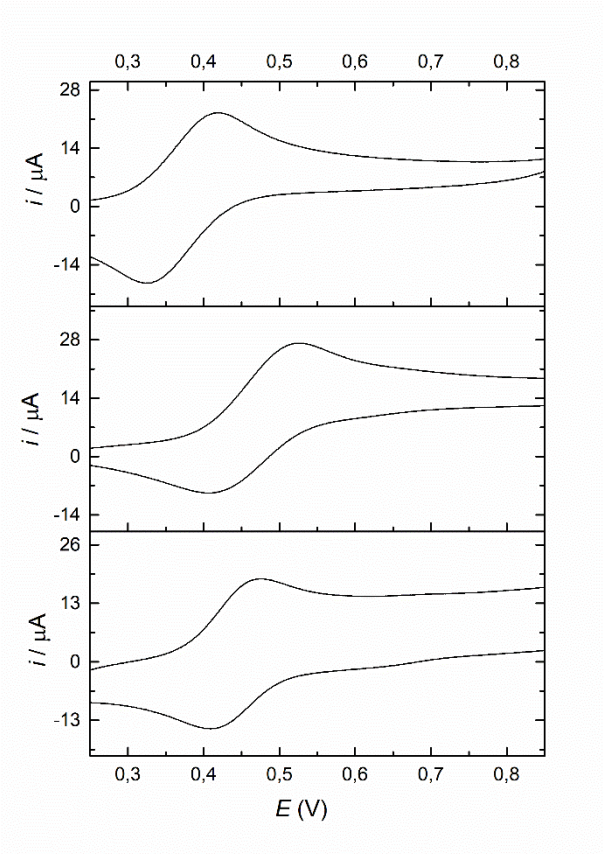

Fig. S13 Cyclic voltammograms of free ferrocene (top), half unit **3** (middle) and of the bimetallic complex **5** (bottom) recorded at a vitreous carbon working electrode in DMF containing 0.1 M [*n*-Bu_4N][PF_6], T = 298 K, v = 100 mV s^{-1}; reference electrode Ag/AgCl.

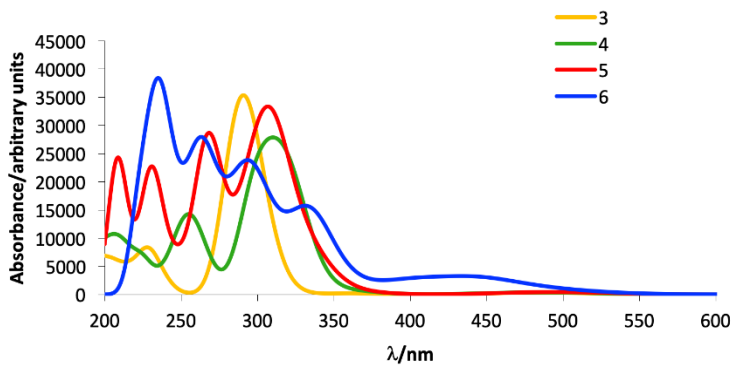

Fig. S14. TD-DFT simulated spectra of complexes **3-6.**

Table S1 Selected metrical parameters of the ferrocenyl units in compounds **3** and **4**·^{i}PrOH.

Compd	Fe-Cp$_{CNT}$ (Å)	Fe-Cp'$_{CNT}$ (Å)	Cp$_{CNT}$-Fe-Cp'$_{CNT}$(°)	Cp/Cp' (°)
3	1.647	1.644	178.0	4.6
4·^{i}PrOH	1.657	1.648	177.6	4.0

Abbreviations: Cp = C_5H_5, Cp' = C_5H_4, CNT = centroid.

Table S2 Hydrogen bond interactions in **3** and **4**·^{i}PrOH.

Compd.	D−H···A	D−H (Å)	H···A (Å)	D···A (Å)	D−H···A (°)
3	N(1)-H···O(1)	0.86	1.962	2.657(4)	137.2
4·^{i}PrOH	N(1)H(1)···O(1)	0.86	2.17	2.675(3)	117.1
	N(2)-H(2B)···O(3)	0.91(4)	2.34(4)	3.205(5)	159(4)
	N(2)-H(2B)···O(3A)	0.91(4)	2.34(4)	3.205(5)	159(4)
	O(2)-H(2)···N(2)$^{\#1}$	0.82	1.87	2.692(4)	175.1
	O(3)-H(3A)···O(1)	0.82	2.04	2.841(4)	165.0
	O(3A)-H(G)···O(1)	0.82	2.10	2.841(4)	149.5

Symmetry transformations used to generate equivalent atoms: #1 x, y, z.